Journal of Solar Energy Research (JSER)

Journal homepage: jser.ut.ac.ir

Design and Investigation of a New Multilevel Inverter with Reduced Number of Semiconductors for Photovoltaic Systems

Hossein Jafari[a,*], Daryoush Nazarpour[a], Sajjad Golshannavaz[a], and Ebrahim Babaei[b]

[a]*Department of Electrical Engineering, Urmia University, Urmia, Iran*
[b]*Department of Electrical Engineering, University of Tabriz, Tabriz, Iran*
Received: 28-04-2021
Accepted: 24-06-2021

Abstract

In this research, a single-phase multilevel inverter with a reduced number of switches and driver circuits is introduced for analysis in photovoltaic systems. The proposed multilevel inverter consists of two parts, basic circuit, and H-bridge, which are responsible for generating voltage levels and symmetry of voltage levels (positive and negative), respectively. The proposed basic circuit in this paper consists of six unidirectional switches and three input sources and doesn't use any capacitors or diodes, which reduces the volume and complexity of the control system. In this paper, the seven-level proposed structure is simulated in the MATLAB/Simulink software and the utilized modulation to generate the output voltage levels is level shifted pulse width modulation. Moreover, photovoltaic systems are exploited to supply the proposed inverter's input sources, which work with perturb and observe algorithm at the maximum power point. In the simulation section, the voltage, current, power waveforms of the photovoltaic system, and the voltage of the proposed inverter input sources are demonstrated, and the voltage and current waveforms of the inverter for different conditions such as radiation and modulation index change are given. Finally, to show the merits and features of the proposed topology, the inverter is compared with some recent symmetrical structures in terms of the number of components and the rated voltage of the switches.

Keywords: Basic Circuit (BC); Symmetric; Maximum Power Point Tracking (MPPT); Perturb and Observe (P&O)

Introduction

In recent years, MLIs have become very popular in high-power applications. Multilevel output voltage in this category of inverters is created by combining several levels of DC voltage. MLIs have lower switching frequency and losses compared to two-level inverters and have higher electromagnetic compatibility (EMC). MLIs play a basic role in high voltage DC (HVDC), induction heating, drive systems, and renewable energy sources [1, 2]. With the presence of MLIs, unregulated power from renewable energy sources is converted into regulated electricity and sent to the consumer. Since the output power quality of MLIs is high and they don't have significant harmonics, so there isn't a need for large and extensive filters [3]. Since MLIs use multiple DC sources, they are suitable for utilized in photovoltaic systems (PVs). PVs are divided into two categories, separate from the grid and connected to the grid. Inverters of PVs are divided into four categories in terms of configuration: central, string, multi-string,

**corresponding author Email address: st_h.jafari@urmia.ac.ir*

and AC module. Central inverter configuration has a simple control system and less power extraction capability. On the other hand, string, multi-string, and AC module inverters have more power generation, modularity, and cost [4, 5]. Inverters with clamp diodes (NPC), flying capacitors (FC), and cascaded H-bridges (CHB) are traditional and industrial structures for MLIs [6]. CHB has the most modularity among MLIs and usually has a simple control system. However, because H-bridge cells are cascaded together to increase the number of output voltage levels, CHB suffers from a large number of power devices [7]. Another category is NPC MLIs, which share the DC link in a three-phase structure and can be used in back-to-back applications. However, a large number of clamp diodes at high voltage levels and neural point voltage deviation usually limit the use of this class of MLIs to five levels [8]. FC is another structure for MLIs, in which the output voltage levels are generated by flying capacitors. FC has also shared the DC link in the three-phase structure and can be a good choice in applications where there is an isolated source imitation. In contrast to the advantages mentioned for FC, the problem of voltage balance of capacitors and the bulkiness and high cost of flying capacitors are FC's limiting parameters for use at high voltage levels [9, 10]. Since the use of power electronic converters in PVs is essential, the design of inverters with higher efficiency and lower cost is one of the important issues [11]. Due to the mentioned limitations in the case of classic inverters, several MLIs have recently been introduced to improve the specifications of MLIs.

One of the recent structures for MLIs is [12]. In this paper, a seventeen-level inverter called st-type has reduced the number of switches compared to conventional structures. The proposed multilevel inverter in this paper has the ability to extend to high voltage levels by cascading the proposed basic modules modularly. Since the total harmonic distortion (THD) of mentioned inverter with one module is obtained in simulation and laboratory 2.77% and 3.06%, respectively, it satisfies the standard of IEEE519. Also, this structure is investigated for various load types that the proposed structure showed its proper performance. Another recent topology for MLIs is [13]. This article presents a hybrid CHB. One of the aims of this article is to reduce the cost of the inverter by reducing the number of switches and driver circuits. This topology has been compared with some current topologies in terms of the cost factor, which shows a reduction in inverter costs. In this article, the THD and efficiency are also tried to be improved. Of course, it should be noted that the proposed inverter efficiency in this article is still low. A new structure with reducing the rated values of the power devices is presented in [14]. This structure is modular and in asymmetric configuration is able to produce seventeen levels. The low-rated voltage values of the utilized devices in the inverter make this structure suitable for high voltage and power applications. Since this structure doesn't use any capacitors, so its dynamic response speed is high and it has a simple control system. one of the challenges of this converter is a large number of semiconductor devices. Another MLI is presented in [15]. This inverter uses an isolated source and several capacitors to increase the number of output voltage levels. This structure doesn't use H-bridge and therefore the total standing voltage (TSV) of it isn't high. The performance of this inverter has been verified by the LS-PWM modulation method in MATLAB/Simulink. One of the challenges of this structure is the high number of switches and driver circuits. [16] is another MLI, which has tried to reduce the number of power devices. In this inverter, a DC voltage source is shared for all three phases, which prevents unbalanced between the phases. An improved PWM is utilized to modulate this inverter so that it prevents over modulation. The related part to the production of levels of this inverter can be extended to the desired number of levels. Despite efforts to reduce the number of devices, this structure still isn't suitable in terms of the utilized power devices. Another new structure is [17]. This structure produces seven and eleven levels in two methods of determining sources symmetrically and asymmetrically, respectively. This structure has been compared with a number of recent structures in terms of devices and costs, which show the comparison results of the superiority of the proposed structure. Of course, it should be noted that despite the efforts made to reduce the number of power devices in this article, the number of components in this converter is still high. Besides, this inverter is both simulated and implemented to validate the proposed circuit.

In this work, in part 2, a basic circuit (BC) with the symmetric determination of voltage sources is presented and combined with an H-bridge to produce all voltage levels symmetrically (positive and negative). Also in this part, a case-study inverter has been selected for simulations. Then, in part 3, the selected modulation method for switching this inverter is studied. Moreover, in section 4, the selected configuration for the PV and the method of performing maximum power point tracking (MPPT) is analyzed. Moreover, In order to validate the inverter performance, the case-study inverter is simulated in MATLAB/Simulink and its output waveforms are demonstrated. Also, in this section, the feasibility of the suggested inverter in the selected PV is investigated. Finally, in order to show the advantage of the introduced inverter, this circuit is compared with CHB and the last three circuits for MLIs in terms of the number of devices (switches, driver circuits, isolated sources), and TSV for the same number of voltage levels.

2. Proposed Circuit

In this section of the paper, according to Fig. 1, a new basic circuit (BC) with the ability to produce positive and zero voltage levels is introduced. This circuit consists of six unidirectional switches and three isolated sources. Due to the high modularity of symmetric structures, these sources have been selected to be equal (V_d). The permissible switching states for this circuit are presented in Table 1. It should be noted that some switching states, such as the simultaneous switching on of S_4 and S_5, leads to a short circuit of some sources and damage to the switches. So these switching states are impermissible and are not listed in Table 1. Moreover, due to the inability to produce negative voltage levels provided by the BC, this circuit is combined with H-bridge to be able to produce all voltage levels symmetrically. Besides, according to Fig. 2 to increase the number of voltage levels, the desired number of BCs are cascaded together and their output is connected to the H-bridge. It should be noted that in Fig. 2, M indicates the cascaded BCs. From the general proposed structure in Fig. 2, a circuit with one BC and H-bridge is selected as a case-study inverter to perform all simulations and other investigations on it. This circuit can generate seven levels on the AC side and is depicted in Fig. 3. The relationship among the number of switches (N_{switch}), driver circuits (N_{driver}), input sources (N_{source}), and TSV with the number of the voltage level on the AC side (N_{level}) are obtained as follows. Also, this converter has been tested for different loads, and the proposed inverter has proved its correct performance.

$$N_{switch} = N_{driver} = N_{level} + 3 \tag{1}$$

$$N_{source} = \frac{(N_{level} - 1)}{2} \tag{2}$$

$$TSV = \frac{19}{6} \times (N_{level} - 1) \tag{3}$$

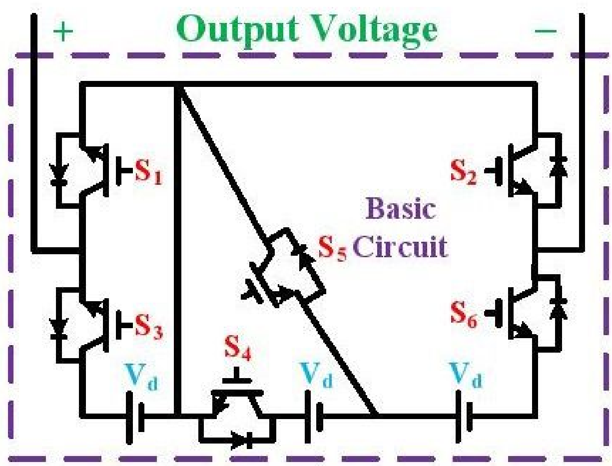

Figure 1. Introduced BC.

Table 1. Accessible switching states for the BC

State	S_1	S_2	S_3	S_4	S_5	S_6	AC Side
1	1	1	0	0	0	0	0
2	0	1	1	0	0	0	V_d
	1	0	0	0	1	1	
3	0	0	1	0	1	1	$2V_d$
	1	0	0	1	0	1	
4	0	0	1	1	0	1	$3V_d$

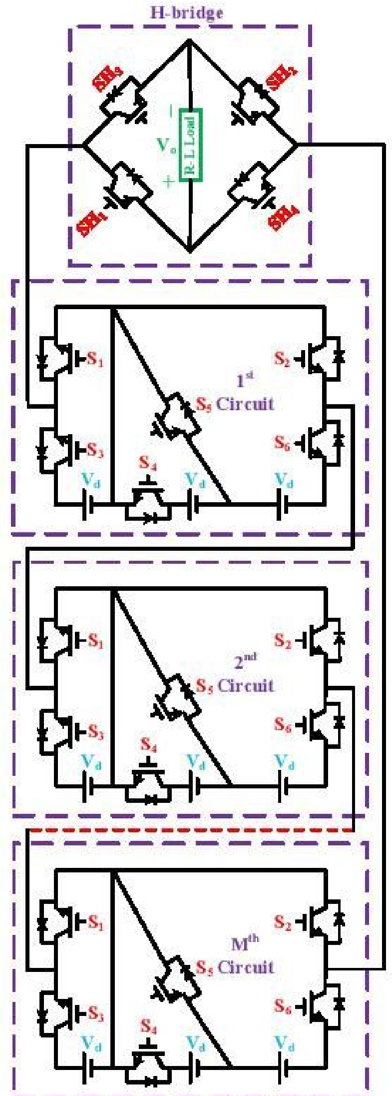

Figure 2. General Configuration of the Introduced Inverter.

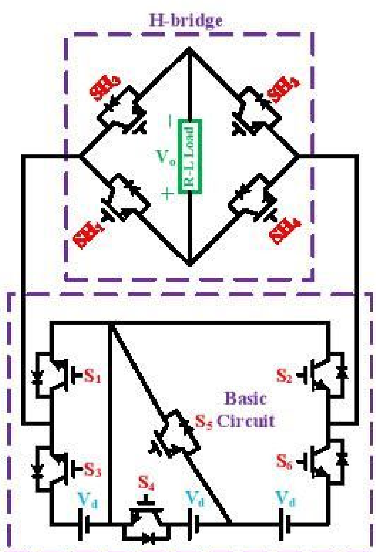

Figure 3. Case-Study Inverter.

3. Modulation Method

There are various modulation methods for switching multilevel inverters to achieve lower output voltage harmonics and switching losses. Different modulation methods in terms of switching frequency fall into three categories: low, medium, and high frequency. The different modulation methods with their examples are shown in Fig. 4. NLC, SHE, and LSPWM are good examples of modulation methods for low, medium, and high frequency, respectively. Also, different modulation methods in terms of switching algorithms are divided into two categories: voltage level-based and space vector-based algorithms [18]. So in this work, in phase disposition LS-PWM (IPD-LSPWM) is selected for generating output voltage levels. In this method, according to Fig. 5, all carrier waveforms are the same amplitude, frequency, and phase and are only at different levels. The frequency of carrier waves is usually several kHz, and to achieve lower output voltage harmonics, the frequency of carrier waves can be increased, which leads to an increase in switching losses. Moreover, in this method, there is a sinusoidal reference voltage with a frequency of 50 or 60 Hz, in which the zero points of it is in the middle of the carrier waveforms and is compared with the carrier waveforms to generate the necessary commands for the inverter switches [19]. The number of carrier waves ($N_{carrier}$) in LS-PWM increases with the increasing N_{level} as provided in equation (4).

$$N_{carrier} = N_{level} - 1 \tag{4}$$

4. Maximum power point tracking algorithm

Extracting the most power from PVs is a necessity. There are several methods for tracking the maximum power point (MPP), each with its own advantages and disadvantages. In PVs, perturb and observe (P&O) and increment conductance methods are usually implemented due to their simplicity. Other maximum power point tracking (MPPT) methods include fuzzy logic-based and neural networks based that track the MPP accurately. Of course, the complexity of implementing these methods is one of their challenges. MPPT methods in terms of the type of radiation are divided into two types, uniform

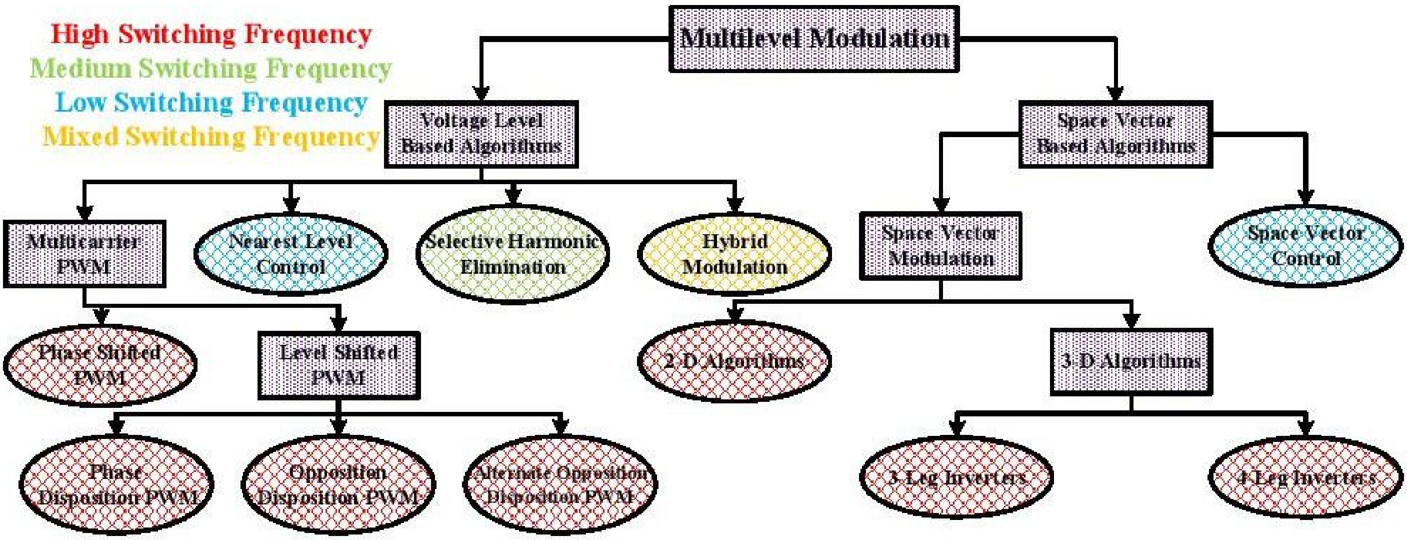

Figure 4. Various MLIs.

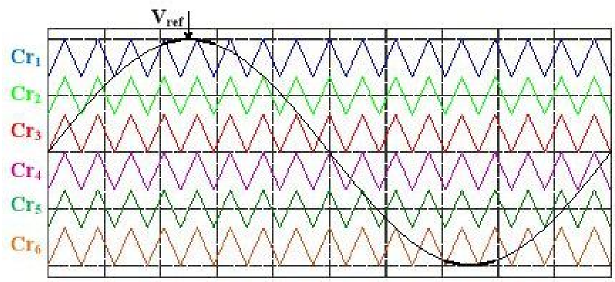

Figure 5. Diagram of IPD-LSPWM.

irradiance, and non-uniform irradiance. Fig. 6 shows some of the famous MPPT methods. Fig. 7 demonstrates the basics of MPPT's performance.

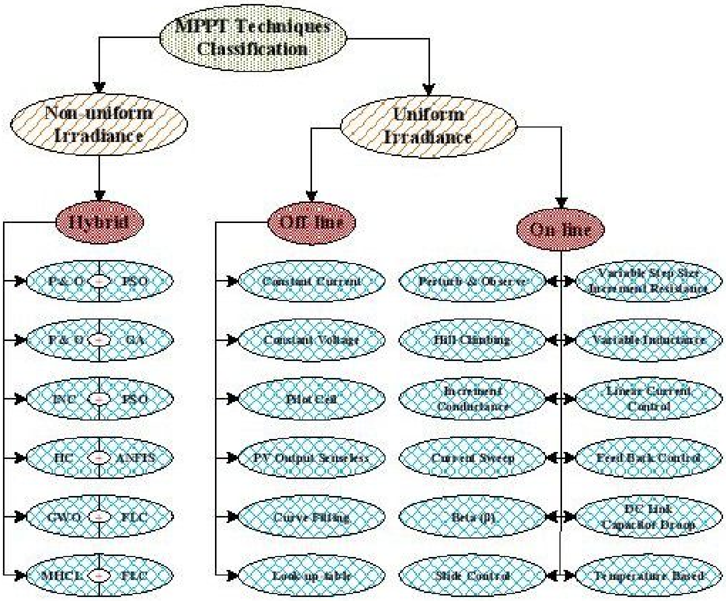

Figure 6. Various MPPTs.

According to this figure, MPPT regulates the voltage and current of the photovoltaic system in such a way that maximum power is extracted from PV. With feedback from PV's voltage and current, MPPT adjusts the duty cycle of the dc-dc converter (boost) to achieve this purpose. The output voltage of the boost converter is then used as the inverter voltage source after being filtered by the capacitor [20, 21].

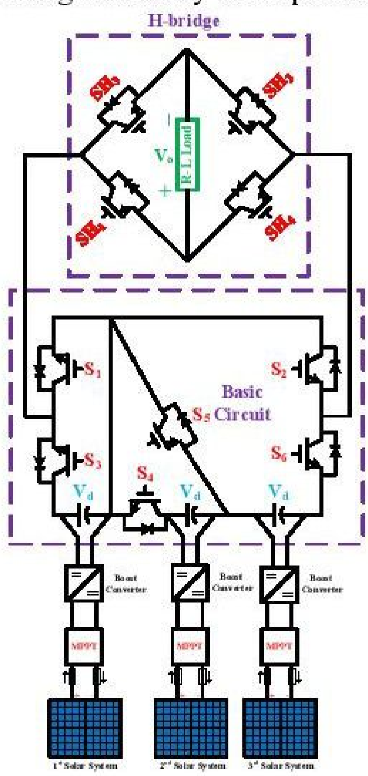

Figure 7. PV with the Centralized Case-Study Inverter.

Since the proposed inverter in this work consists of three isolated sources, each of the sources, as shown in Fig. 7, is supplied by one of the PVs. In this work, the P&O method has been selected for MPPT due to the simplicity of the control system and implementation. This method is a process in which a variable disturbs and the effect of that disturb on other variables is observed. The diagrams in Fig. 8 show the points on the I-V and P-V curves of the PV to which the P&O is applied. In this method, the output voltage on the I-V curve is shifted to change the module load. This process continues until it reaches the maximum power point. The MPPT method starts with adjusting the amount of load and measuring V_1 and output current. P_1 is measured at the point of V_1. Then, the load increased and the amount of P_2 is observed at the point of V_2. The amount of P_2 is compared to P_1, and since P_2 is bigger than P_1, the MPPT continues to change in the same direction. This process continued until P_4 and due to P_5 is smaller than P_4, the working point returned to P_4. The accuracy of this method depends on the value of voltage changes, so smaller changes will result in more accuracy in MPPT [22]. The performance flowchart of the P&O method is shown in Fig. 9 so that the disturbance and observation continue until the maximum power point is reached.

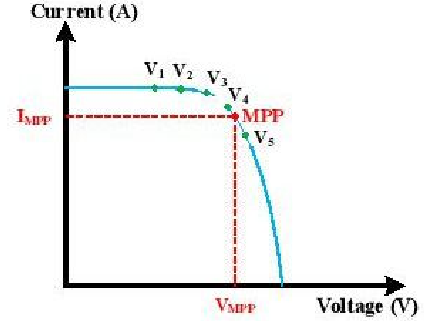

(a)

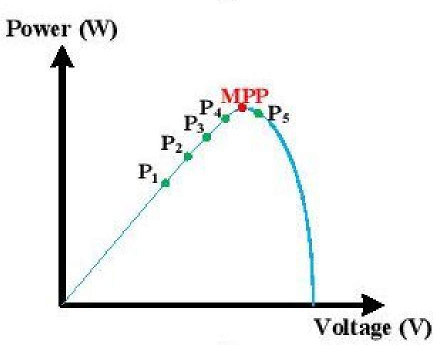

(b)

Figure 8. (a) I-V (b) P-V Curves of the PV.

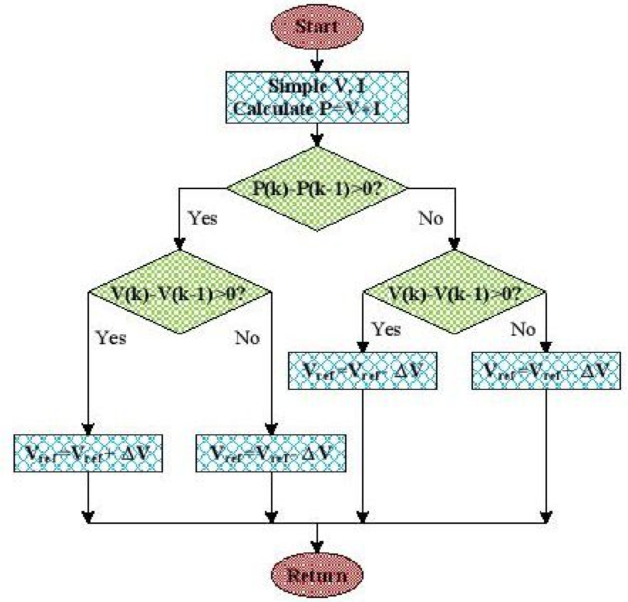

Figure 9. Diagram of P&O Method Performance.

5. Simulation Results

To show the correct performance and feasibility of the proposed structure, the suggested inverter is simulated in MATLAB/Simulink and the output of it is provided in Fig. 10. The simulation characteristics are provided in Table 2. It should be noted that the

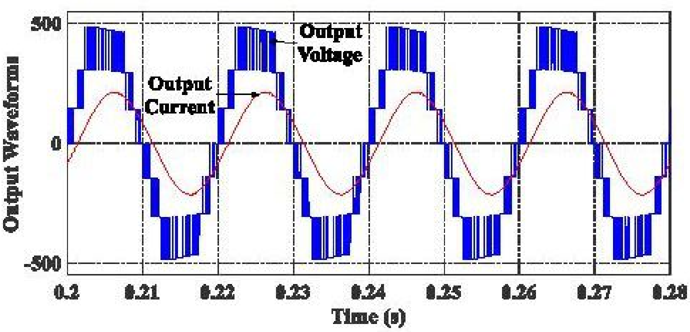

Figure 10. The Output of the Case-Study Inverter.

Table 2. Characteristics of the simulation

Character	Value
Carrier Waveforms Frequency	3 kHz
Reference Waveform Frequency	50 Hz
Load	Resistance=20Ω, and Inductance=30mH
Power Factor	0.9
Modulation Index	1

current waveform has been increased 10 times to be clearly shown in all simulations. So that the voltage sources of this inverter are supplied by solar cells. The characteristics of each PV that supplied one of the introduced inverter sources are given in Table 3. Moreover, Fig. 11 demonstrates the fast fourier transform (FFT) of the inverter output voltage.

Table 3. Characteristics of the utilized photovoltaic system

Character	Value
Irradiance	1000 w/m^2
Temperature	25°c
K_V	-0.123/32.9 %/°
K_i	3.18e-3/8.21 %/°
I_{sc}	8.21
V_{oc}	32.9
R_s	0.2172 Ω
R_{sh}	951.9317 Ω
Number of Serie Modules	3
Number of Parallel Modules	3
Rated Power of Each Modules	200 W

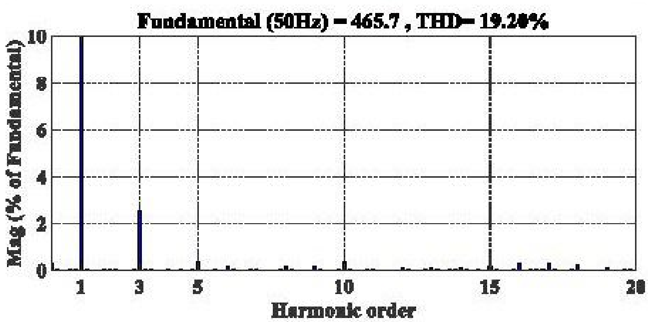

Figure 11. FFT of the Case-Study Inverter Voltage.

Besides, PV voltage (V_{PV}), PV current (I_{PV}), PV power (P_{PV}), and input sources voltage (V_d) waveforms are demonstrated in Fig. 12. Furthermore, the P_{PV}-V_{PV} and I_{PV}-V_{PV} curves for the utilized PV are

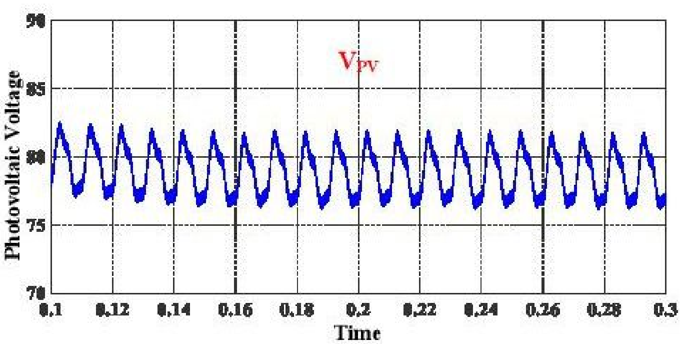

(a)

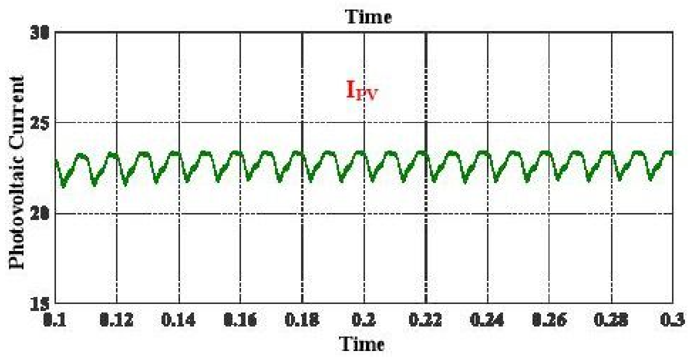

(b)

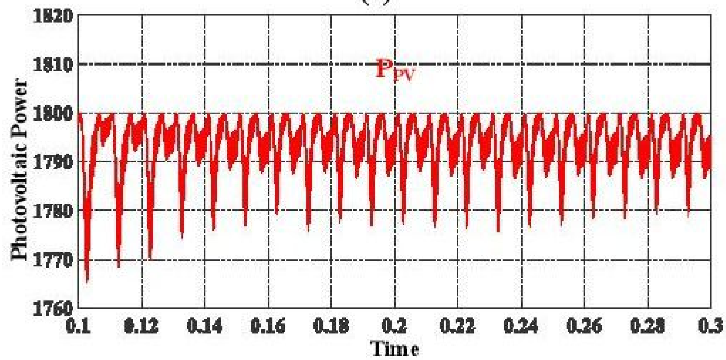

(c)

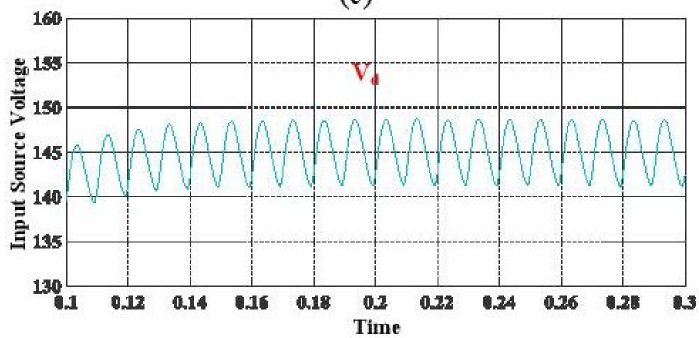

(d)

Figure 12. (a) V_{PV} (b) I_{PV} (c) P_{PV} (d) V_d Waveforms.

illustrated in Fig. 13. According to these curves, it is clear that MPPT is working properly and that the PVs

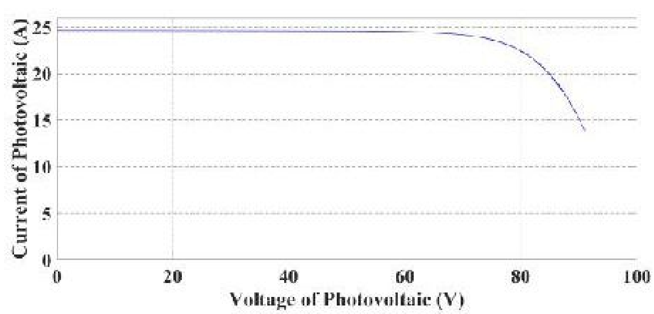

(a)

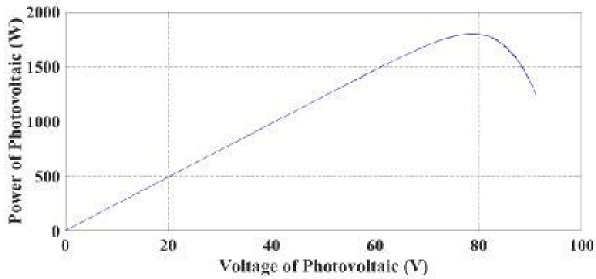

(b)

Figure 13. (a) I-V (b) P-V Curves of the Simulated PV.

are working in the knee area of the curve. For further study and also to investigate the possibility of the proposed inverter of operation in different conditions, the output waveforms of the proposed structure by changing the conditions in t=0.24s are provided in Fig. 14.

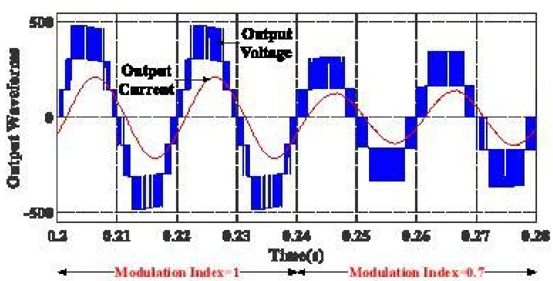

(a)

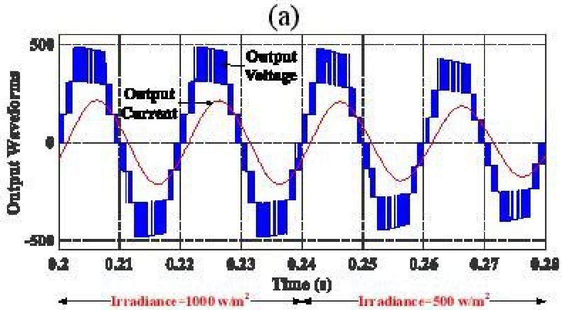

(b)

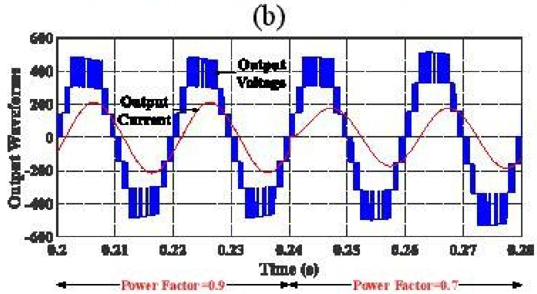

(c)

Figure 14. The Output of the Case-Study Inverter for Changing (a) Modulation Index (b) Irradiance (c) Load.

6. Comparison

In this section, to show the superiority of the proposed circuit over other MLI structures, this circuit is compared with CHB and some currently structures with symmetrically determination input sources, in terms of the number of power devices (N_{switch}, N_{driver}, N_{source}), and TSV for the same N_{level}. Since the number of devices and the amount of reverse voltage on the switches play the main role in determining the total cost of the inverter and the complexity of the MLI control system, researchers always try to have the least number with lower-rated voltage values for generating more voltage levels. According to Fig. 15 (a), the proposed structure (P) in terms of the N_{switch} and N_{driver} is better than CHB and [15-17], indicated R1-R3. Moreover, Fig. 15 (b) compares the symmetrical structures of MLIs in terms of the N_{source}, which according to this figure, the proposed structure utilizes fewer input sources than R2 and equal to CHB. Besides, as shown in Fig. 15 (c), since the proposed circuit uses H-bridge in its output, the TSV of it is high and only lower than R1. Therefore,

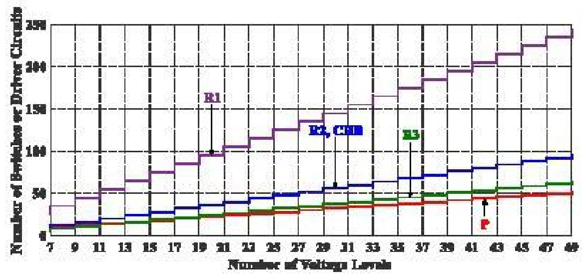

(a)

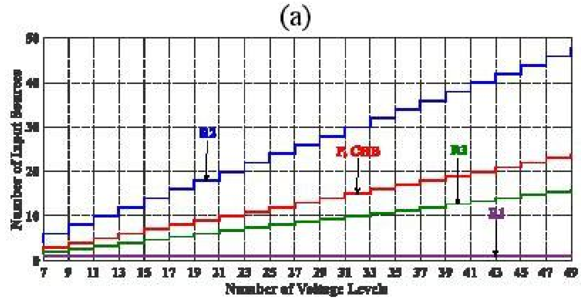

(b)

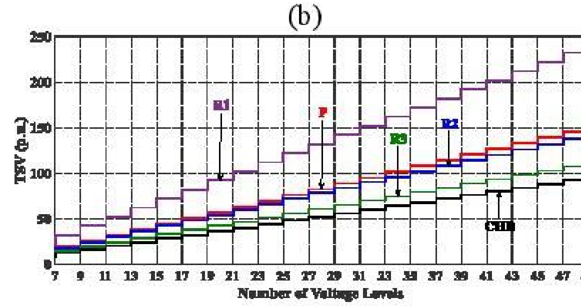

(c)

Figure 15. Comparison of Recent MLIs in the Viewpoint of (a) N_{switch} or N_{driver} (b) N_{source} (c) TSV.

according to Fig. 15 (b) and Fig. 15 (c), it is concluded that the proposed structure in terms of the N_{source} and TSV is in the middle range and acceptable.

7. Conclusion

In this research, a multilevel inverter with the approach of reducing the number of power devices for utilization in photovoltaic systems was presented. By combining with H-bridge, this inverter was able to produce all voltage levels symmetrically and was able to extend to high voltage levels by cascading more basic circuits. Since the modularity of the inverter is an important issue in the industry, so this inverter was utilized only symmetrically. Then the IPD-LSPWM modulation strategy was utilized to provide suitable power quality. In order to investigate the feasibility and prove the proper performance of the proposed inverter, it is simulated for photovoltaic systems in MATLAB/Simulink software and different waveforms for different conditions such as change radiation and load are shown. In the simulation section, the photovoltaic systems were operated at maximum power point by the perturb and observe algorithm and their output voltage after the increased by boost converters, exploited as the proposed inverter input sources. Finally, to prove the superiority of the proposed structure, this inverter was compared with some new MLI structures in terms of the number of devices and TSV, which showed a satisfactory result.

References

1. Meraj, M., et al., *Novel Level-Shifted PWM Technique for Equal Power Sharing Among Quasi-Z-Source Modules in Cascaded Multilevel Inverter*. IEEE Transactions on Power Electronics, 2020. **36**(4): p. 4766-4777.
2. Jafari, H., et al. *Design and Analysis of a New Multilevel Inverter with Reduced Number of Switching Devices*. in *2021 12th Power Electronics, Drive Systems, and Technologies Conference (PEDSTC)*. 2021. IEEE.
3. Liang, W., Y. Liu, and J. Peng, *A Day and Night Operational Quasi-Z Source Multilevel Grid-Tied PV Power System to Achieve Active and Reactive Power Control*. IEEE Transactions on Power Electronics, 2020. **36**(1): p. 474-492.
4. Nazer, A., et al., *Optimal Photovoltaic Multi-String Inverter Topology Selection Based on Reliability and Cost Analysis*. IEEE Transactions on Sustainable Energy, 2020.
5. Karanayil, B., S. Ceballos, and J. Pou, *Maximum power point controller for large-scale photovoltaic power plants using central inverters under partial shading conditions*. IEEE Transactions on Power Electronics, 2018. **34**(4): p. 3098-3109.
6. Jafari, H., et al. *A New Hybrid Three-Phase Multilevel Inverter Devoted to Electric Drive with Constant Volt per Hertz Control*. in *2021 12th Power Electronics, Drive Systems, and Technologies Conference (PEDSTC)*. 2021. IEEE.
7. Ramos, E.R., et al., *Incremental Passivity Control in Multilevel Cascaded H-Bridge Converters*. IEEE Transactions on Power Electronics, 2020. **35**(8): p. 8766-8778.
8. Wang, K., et al., *Neutral-point voltage balancing method for five-level NPC inverters based on carrier-overlapped PWM*. IEEE Transactions on Power Electronics, 2020. **36**(2): p. 1428-1440.
9. Ebrahimi, J. and H. Karshenas, *A new modulation scheme for a four-level single flying capacitor converter*. IEEE Transactions on Industrial Electronics, 2020. **68**(3): p. 1860-1870.
10. Kan, S., et al., *Second harmonic current reduction for flying capacitor clamped boost three-level converter in photovoltaic grid-connected inverter*. IEEE Transactions on Power Electronics, 2020. **36**(2): p. 1669-1679.
11. Khasim, S.R., et al., *A Novel Asymmetrical 21-Level Inverter for Solar PV Energy System With Reduced Switch Count*. IEEE Access, 2021. **9**: p. 11761-11775.
12. Samadaei, E., et al., *A square T-type (ST-Type) module for asymmetrical multilevel inverters*. IEEE Transactions on power Electronics, 2017. **33**(2): p. 987-996.
13. Dhanamjayulu, C., et al., *Design and Implementation of Seventeen Level Inverter With Reduced Components*. IEEE Access, 2021. **9**: p. 16746-16760.
14. Kakar, S., et al., *New Asymmetrical Modular Multilevel Inverter Topology With*

Reduced Number of Switches. IEEE Access, 2021. **9**: p. 27627-27637.

15. Taghvaie, A., J. Adabi, and M. Rezanejad, *A self-balanced step-up multilevel inverter based on switched-capacitor structure*. IEEE Transactions on Power Electronics, 2017. **33**(1): p. 199-209.
16. Hota, A., S. Jain, and V. Agarwal, *An optimized three-phase multilevel inverter topology with separate level and phase sequence generation part*. IEEE Transactions on Power Electronics, 2017. **32**(10): p. 7414-7418.
17. Selvaraj, S., G. Kumaresan, and M.A.J. Sathik, *Modified "K" -type multilevel inverter topology with reduced switches, DC sources, and power loss*. International Transactions on Electrical Energy Systems, 2020. **30**(5): p. e12345.
18. Poorfakhraei, A., M. Narimani, and A. Emadi, *A review of modulation and control techniques for multilevel inverters in traction applications*. IEEE Access, 2021. **9**: p. 24187-24204.
19. Iqbal, A., et al., *Experimental investigation and comparative evaluation of standard level shifted multi-carrier modulation schemes with a constraint GA based SHE techniques for a seven-level PUC inverter*. IEEE Access, 2019. **7**: p. 100605-100617.
20. Bollipo, R.B., S. Mikkili, and P.K. Bonthagorla, *Hybrid, optimal, intelligent and classical PV MPPT techniques: A review*. CSEE Journal of Power and Energy Systems, 2020. **7**(1): p. 9-33.
21. Kumar, P., R.K. Singh, and R. Mahanty, *Performance of MPPT-Based Minimum Phase Bipolar Converter for Photovoltaic Systems*. IEEE Transactions on Power Electronics, 2020. **36**(5): p. 5594-5609.
22. Zhang, X., et al., *Hybrid Maximum Power Point Tracking Method Based on Iterative Learning Control and Perturb & Observe Method*. IEEE Transactions on Sustainable Energy, 2020. **12**(1): p. 659-670.